176
10/15/79

DR-150

GA-A15141
UC-77

MASTER

INFLUENCES OF THE COUPLE-STRESSES ON THE PURE-BENDING OF A CIRCULAR CYLINDER

by
B. G. KAO, F. K. TZUNG, and F. H. HO

Prepared under
Contract DE-AT03-76ET35300
for the San Francisco Operations Office
Department of Energy

DATE PUBLISHED: JULY 1979

GENERAL ATOMIC COMPANY

DISCLAIMER

Printed in the United States of America
Available from
National Technical Information Service
U.S. Department of Commerce
5285 Port Royal Road
Springfield, Virginia 22161
Price: Printed Copy $4.50; Microfiche $3.00

GA-A15141
UC-77

INFLUENCES OF THE COUPLE-STRESSES ON THE PURE-BENDING OF A CIRCULAR CYLINDER

by
B. G. KAO, F. K. TZUNG, and F. H. HO

Prepared under
Contract DE-AT03-76ET35300
for the San Francisco Operations Office
Department of Energy

GENERAL ATOMIC PROJECT 6400
DATE PUBLISHED: JULY 1979

GENERAL ATOMIC COMPANY

ABSTRACT

This report presents the solution to the pure-bending of a circular cylinder with the couple-stress theory of linear elasticity. A linear bending moment-curvature relation is derived parallel to the classical beam theory. The section modulus (or the proportional coefficient) associated with the couple-stress theory is always greater than that predicted by the classical theory, and the ratio of the former to the latter increases as the radius of the beam decreases. These aspects clearly agree with the observed behavior of nuclear-grade graphite.

Based on the solution, it is further estimated that the characteristic length ℓ_2 of the couple-stress theory for H-451 graphite ranges from 0.62 to 1.54 mm. This range of ℓ_2 concurs with the magnitude of the grain size (maximum is 1.57 mm for H-451 graphite) and agrees with an aspect of the couple-stress theory.

NOMENCLATURE

$[\![\ ]\!]$	difference of the quantity across the edge of C
$(\underset{\sim}{\ })$	vector or tensor
$(\ )_{,i}$	component of $(\underset{\sim}{\ })$; partial derivative with respect to x_i
A	cross section
A_2, B_2 ...	constants of integration
a	radius of the cylinder; radius of the cylindrical beam
B	couple-stress medium
C	edge
C_m	coefficient of bending moment; moment coefficient; quadratic function of $\bar{d}_2$
C_t	coefficient of axial flexural stress; stress coefficient; linear function of $\bar{d}_2$
$\bar{d}_1$, $\bar{d}_2$	couple-stress constants
$d\ell$, ds, dv	line, surface, and volume area elements, respectively
E	Young's modulus
$\underset{\sim}{\bar{E}}$	applied force on edge C of the bounding surface
e_{jkl}	permutation symbol (used with summation convention jkl, jpq, lpq, etc.)
$I_n(\ )$, $K_n(\ )$	modified Bessel functions of the first and second kinds, respectively
i, j, k, l p, q	summation over the range of the indices 1, 2, 3; summation convention is adopted, unless otherwise noted
ℓ_2	material parameter, characteristic length of the couple-stress theory for H-451 graphite; defined by Eq. 2-3
$\underset{\sim}{M}$, M_x, M_y	bending moment vector and components of the bending moment about x-axis and y-axis, respectively

$\underset{\sim}{m}_{\underset{\sim}{n}}$	surface couple
$\underset{\sim}{n}$	surface of unit outward normal vector
P	partition
$\underset{\sim}{\bar{P}}$	applied surface force
$\underset{\sim}{\bar{Q}}$	tangential surface couple
r, $\underset{\sim}{r}$	position and position vector, respectively
$\underset{\sim}{t}$	unit tangent vector along edge of bounding surface
$\underset{\sim}{t}_{\underset{\sim}{n}}$	surface force
u, $\underset{\sim}{u}$	displacement field and displacement field vector, respectively; plane strain displacement
$\underset{\sim}{u}^{(1)}$	secondary deformation field, displacement
w, $\underset{\sim}{w}$	rotation and rotation vector, respectively
x_1, x_2, x_3	cartesian coordinates
∇	differential operator
$\nabla\cdot$	divergence
∇x	curl
δ_{ij}	Kronecker delta function
$\delta\underset{\sim}{u}$	virtual displacement
δw	rotation accompanying $\delta\underset{\sim}{u}$
$\delta\underset{\sim}{\varepsilon}$	strain gradient associated with virtual displacement
$\delta\underset{\sim}{\kappa}$	rotation gradient associated with virtual displacement
$\underset{\sim}{\varepsilon}$	strain tensor, kinematic quality of couple-stress theory
$\underset{\sim}{\kappa}$	rotation gradient tensor; kinematic quality of couple-stress theory; length inverse
λ, μ	Lame' constants
$\underset{\sim}{\mu}$	couple-stress tensor; plane strain displacement

$\overline{\underset{\sim}{\mu}}$	deviatory part of $\underset{\sim}{\mu}$; linear isotropic function of $\underset{\sim}{\kappa}$; moment per unit area
μ_{kk}	trace of $\underset{\sim}{\mu}$, scalar function
ν	Poisson's ratio
$\underset{\sim}{\tau}$	stress tensor
$\underset{\sim}{\tau}^{A}$	skew-symmetric part of $\underset{\sim}{\tau}$
$\underset{\sim}{\tau}^{S}$	symmetric part of $\underset{\sim}{\tau}$, linear isotropic function of $\underset{\sim}{\varepsilon}$
τ_{zz}	axial stress
$\tau_{zz}^{(a)}$	apparent flexural stress
∂P	surface enclosing P

CONTENTS

FIGURES

1. INTRODUCTION

This report studies the implications of the couple-stress theory of linear elasticity in modelling the mechanical behavior of granular brittle materials, specifically the graphite used in gas-cooled nuclear reactors. It solves a boundary value problem and then compares the results with the laboratory-observed phenomena of graphite.

The complete boundary value problem in couple-stress theory of linear elasticity was first correctly formulated by Mindlin and Tiersten (Ref. 1). The general aspects of this theory, as described by Mindlin (Ref. 2), are that

1. The couple-stress influence depends strongly on the ratio of the smallest dimension of the body to the material parameter ℓ_2 (defined by Eq. 2-13).

2. If the ratio is large, the couple-stress effect is negligible.

3. When there are strain gradients and a dimension of a body approaches ℓ_2, couple-stresses may produce effects of appreciable magnitude.

4. The material parameter ℓ_2 is related to and believed to be about the same order of magnitude as the grain size for idealized granular materials.

In general, the laboratory mechanical test data of graphite show that, in the presence of strain gradients, the apparent stress and apparent strength, calculated by classical elasticity, consistently exceed the stress and the strength determined by the homogeneous deformations (Ref. 3).

For instance, in the pure-bending test of a graphite beam, the apparent flexural stress (as defined in Eq. 7-1) at any given strain exceeds the uniaxial tensile stress by approximately 35%, and the apparent flexural strength exceeds the uniaxial tensile strength by nearly 50% (Ref. 3). This phenomenon contradicts the constitutive assumption of classical elasticity that the mechanical responses are uniquely determined by the strain. Rather, it shows that the strain gradients affect the mechanical responses of graphite. Moreover, Brocklehurst (Ref. 4) perceived that "the influence of grain size relative to specimen dimensions must be considered when obtaining strength data on different (graphite) materials." He points out that the apparent flexural strength is dependent on the same parameter, the ratio of the smallest dimension to grain size (in lieu of ℓ_2) as is the couple-stress theory. These evidences make clear that the mechanical responses of the graphite and the couple-stress theory have many similarities, leading to the assumption that the mechanical responses of graphite reflect couple-stress influence. This assumption and the dimensional argument furnished in Ref. 2, quoted earlier, are used below to estimate the error caused by neglecting couple-stresses when analyzing laboratory pure-bending test data.

The pure-bending test data of graphite show that most test specimens are cylinders with the smallest dimension approximately 10 mm and with the maximum grain sizes ranging from 0.4 to 6.7 mm (Ref. 3). The ratio of the smallest dimension to the grain size for most of the test specimens is on the order of 10. This is not a large enough number to indiscriminately neglect the couple-stress influence without further investigation of the problem. To quantitatively establish the couple-stress effects on the mechanical behavior of graphite beams, the solution of the boundary value problem for a circular cylinder under pure-bending is pursued further and then compared with the existing experimental data.

The governing equations of the couple-stress theory for an isotropic linear elastic medium and the accompanying boundary conditions are reproduced in Section 2 following the work of Mindlin and Tiersten (Ref. 1). The formulae of stress and couple-stress are also derived. The solution

for the pure-bending of a circular cylinder is then formulated in Sections 3 and 4 by superimposing a plane strain deformation to the classical linear elastic solution. The assumption in classical pure-bending solution (that the normal cross section of the beam remains in a plane) is preserved in the solution obtained in this report.

In Section 5, the solution is used in calculating the stress field, the couple-stress field, and the bending-moment for a given bending curvature. Numerical results of the bending-moment and the axial tensile stress as functions of a/ℓ_2 (a is the radius of the cylinder) are also presented for given values of Poisson's ratio. These results are summarized in Section 6.

The theoretical results of the couple-stress theory and the experimentally observed phenomena of graphite are qualitatively compared in Section 7. Most observed phenomena on graphite beams under pure-bending tests which disagree with the classical elasticity and the uniaxial tensile test results can be satisfactorily interpreted by the solution of the couple-stress theory presented in this report.

The dimensional argument for the couple-stress theory is also employed to estimate the characteristic length ℓ_2 according to the solution and a measured result for a graphite. This procedure yields a range of ℓ_2 that concurs with the magnitude of grain size for the graphite and clearly complies with the observation that ℓ_2 is at the same order magnitude as grain size.

2. COUPLE-STRESS THEORY OF LINEAR ELASTICITY

In this section, an outline of the couple-stress theory of linear elasticity for isotropic materials, derived by Mindlin and Tiersten (Ref. 1), is presented. Since the concern in this report is the static equilibrium state between loading and deformation, the body forces, body couple-forces, and inertia are all neglected in the formulation of this section. Tensorial index notation and the rectangular cartesian coordinate system x_1, x_2 x_3, are predominantly employed in this section.

For any partition P of a couple-stress medium B (see Fig. 2-1) with no body forces and body couples, the equations of equilibrium are

$$\int_{\partial P} \underset{\sim}{t}_{(\underset{\sim}{n})} \, ds = 0 \quad , \tag{2-1a}$$

$$\int_{\partial P} \left(\underset{\sim}{m}_{(\underset{\sim}{n})} + \underset{\sim}{r} \underset{\sim}{x} \, \underset{\sim}{t}_{(\underset{\sim}{n})} \right) ds = 0 \quad , \tag{2-1b}$$

where ∂P = surface enclosing P,

$\underset{\sim}{t}_{(\underset{\sim}{n})}$ = surface force,

$\underset{\sim}{m}_{(\underset{\sim}{n})}$ = surface couple,

ds = surface area element,

$\underset{\sim}{r}$ = position vector, and

$\underset{\sim}{n}$ = unit outward normal vector.

Taking P as a tetrahedron enclosed by a surface of unit normal $\underset{\sim}{n}$ and the planes parallel to the coordinate planes in the rectangular cartesian coordinate system, then letting the volume of the tetrahedron shrink to zero, results in Eq. 2-1 yielding

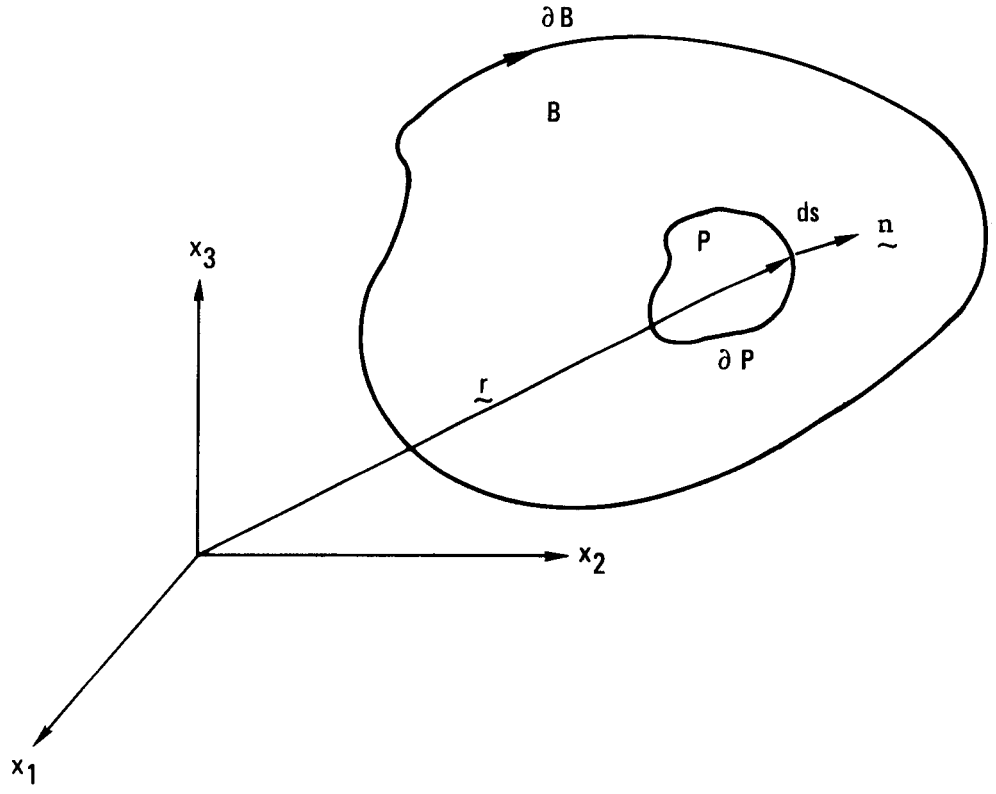

Fig. 2-1. Partition P of a couple-stress medium B

$$t_{(n)i} = n_j \tau_{ji}$$

$$m_{(n)i} = n_j \mu_{ji} \quad , \qquad (i, j = 1, 2, 3) \tag{2-2}$$

where $\underset{\sim}{\tau}$ = the stress tensor,

$\underset{\sim}{\mu}$ = the couple-stress tensor, and the repeated indices

i and j = the summation over the range of the indices (adopting the summation convention).

Substituting Eq. 2-2 back into Eq. 2-1 and applying the divergence theorem provides

$$\tau_{ij,i} = 0 \quad , \tag{2-3a}$$

$$\mu_{ij,i} + e_{jkl} \tau_{kl} = 0 \quad , \qquad (i, j, k, 1, = 1, 2, 3) \tag{2-3b}$$

where $(\ )_{,i}$ = the partial derivative with respect to x_i, and

e_{jkl} = the permutation symbol.

Equation 2-3a is the familiar equation of equilibrium, but Eq. 2-3b relates the couple-stress $\underset{\sim}{\mu}$ with the skew-symmetric part of $\underset{\sim}{\tau}$ (shown as $\underset{\sim}{\tau}^A$ in Eq. 1-4 below). If Eq. 2-3b is multiplied by the permutation tensor e_{jpq} and the sum over j, then

$$\tau^A_{pq} = -\frac{1}{2} e_{jpq} \mu_{lj,l} \quad , \qquad (p,q = 1, 2, 3) \tag{2-4}$$

where τ^A_{pq} = the component of $\underset{\sim}{\tau}^A$.

Let $\underset{\sim}{\mu}$ be represented by the partition

$$\mu_{ij} = \bar{\mu}_{ij} + \frac{\delta_{ij}}{3} \mu_{kk} \quad , \tag{2-5}$$

where δ_{ij} = the Kronecker delta function,

$\underset{\sim}{\bar{\mu}}$ = the deviatory part of $\underset{\sim}{\mu}$, and

μ_{kk} = the trace of $\underset{\sim}{\mu}$.

Then Eqs. 2-3, 2-4, and 2-5 and

$$e_{lpq}\ \mu_{kk,lp} = 0$$

yield

$$\tau^{S}_{ij,i} - \frac{1}{2}\ e_{kij}\ \bar{\mu}_{lk,li} = 0 \quad , \tag{2-6}$$

where $\underset{\sim}{\tau}^{S}$ = the symmetric part of $\underset{\sim}{\tau}$.

The scalar function μ_{kk} of Eq. 2-5 is an important function in satisfying the traction boundary conditions. However, since it does not appear in the equation of equilibrium, it is a function of position but does not influence the equilibrium equations. As a result, adoption of the convention

$$\mu_{kk} = 0 \quad , \tag{2-7}$$

is possible, and the boundary conditions that involve μ_{kk} can be determined later. With this convention, the stress tensor becomes

$$\tau_{ij} = \tau^{S}_{ij} - \frac{1}{2}\ e_{pij}\ \bar{\mu}_{lp,l} \quad . \tag{2-8}$$

Now the linear isotropic elastic solids are concentrated, and the constitutive assumptions of the couple-stress theory of linear elasticity are recorded. The kinematic quantities of the couple-stress theory are defined as

$$\varepsilon_{ij} = \frac{1}{2}\left(u_{i,j} + u_{j,i}\right) \quad , \tag{2-9a}$$

$$w_k = \frac{1}{2} e_{kij} u_{j,i} \quad , \tag{2-9b}$$

$$\kappa_{ij} = w_{j,i} \quad , \tag{2-9c}$$

where $\underset{\sim}{\varepsilon}$ = the strain tensor,

$\underset{\sim}{\kappa}$ = the rotation gradient tensor,

$\underset{\sim}{u}$ = a given displacement field, and

$\underset{\sim}{w}$ = the rotation vector.

Inspection of Eqs. 2-5, 2-7, and 2-8 indicates that at least constitutive assumptions for $\underset{\sim}{\tau}^S$ and $\underset{\sim}{\bar{\mu}}$ in the couple-stress theory of linear elasticity are needed. For the isotropic elastic media, it is assumed that $\underset{\sim}{\tau}^S$ and $\underset{\sim}{\bar{\mu}}$ are linear isotropic functions of $\underset{\sim}{\varepsilon}$ and $\underset{\sim}{\kappa}$, respectively:

$$\tau^S_{ij} = \lambda\varepsilon_{kk}\delta_{ij} + 2\mu\varepsilon_{ij} \quad , \tag{2-10a}$$

$$\bar{\mu}_{ij} = 4\bar{d}_1 \kappa_{ij} + 4\bar{d}_2 \kappa_{ji} \quad , \tag{2-10b}$$

where λ and μ = the Lamé constants, and $\bar{d}_1$ and $\bar{d}_2$ = the couple-stress constants. Dimensionally, since $\underset{\sim}{\bar{\mu}}$ is moment per unit area and $\underset{\sim}{\kappa}$ is length inverse, $\bar{d}_1$ and $\bar{d}_2$ have the unit of force. In Eq. 2-10b, since $\kappa_{kk} = 0$ from Eqs. 2-9b and 2-9c, $\underset{\sim}{\bar{\mu}}$ is trace free and is, hence, the deviator of the couple-stress $\underset{\sim}{\mu}$.

The positive-definiteness of the strain-energy requires that λ, μ, $\bar{d}_1$, and $\bar{d}_2$ satisfy the restrictions (Ref. 1)

$$\mu > 0 \quad , \qquad 3\lambda + 2\mu > 0 \quad ,$$

$$\bar{d}_1 > 0 \quad , \qquad \bar{d}_1 > \bar{d}_2 > -\bar{d}_1 \quad . \tag{2-11}$$

It is assumed in this report that Eq. 2-11 is met for the material constants.

The equation of equilibrium (Eq. 2-6) can be expressed in terms of the displacement field $\underset{\sim}{u}$ by using Eqs. 2-9 and 2-10. In vector notation, it is

$$(\lambda + 2\mu)\ \nabla\nabla\cdot \underset{\sim}{u} - \mu(1 - \ell_2^2\ \nabla^2)\ \nabla x\ \nabla x\ \underset{\sim}{u} = 0 \quad , \tag{2-12}$$

where ∇ = the differential operator,

$\nabla\cdot$ = divergence,

∇x = curl, and

ℓ_2 = the characteristic length defined by

$$\ell_2^2 = \bar{d}_1/\mu \quad . \tag{2-13}$$

To determine the solutions for Eqs. 2-9, 2-10, and 2-12 in the surface traction boundary value problems requires knowing the conditions on the boundary that relate the surface traction to the internal stress and couple-stress. A short review of the boundary conditions derived by Mindlin and Tiersten (Ref. 1) follows.

For an arbitrary admissible variation $\delta\underset{\sim}{u}$ of the displacement field $\underset{\sim}{u}$ in the body B, the principle of virtual work requires that

$$\int_B \left(\tau^S_{ij}\ \delta\varepsilon_{ij} + \bar{\mu}_{ij}\ \delta\kappa_{ij}\right) dv = \int_{\partial B} \left(\bar{P}_i\ \delta u_i + \bar{Q}_i\ \delta w_i\right) ds + \int_C \bar{E}_i\ \delta u_i\ d\ell \quad , \tag{2-14}$$

where the left-hand side = the variation of the strain-energy caused by the virtual displacement $\delta\underset{\sim}{u}$,

$\delta\underset{\sim}{\varepsilon}$ and $\delta\underset{\sim}{\kappa}$ = the strain gradient and the rotation gradient, respectively, associated with the virtual displacement, and

dv = the volume area element.

On the right-hand side,

$\bar{\underset{\sim}{P}}$ = the applied surface force,

$\bar{\underset{\sim}{Q}}$ = the tangential surface couple,

$\bar{\underset{\sim}{E}}$ = the applied force on the edge C of the bounding surface,

$\delta\underset{\sim}{w}$ = the rotation accompanying $\delta\underset{\sim}{u}$, and

$d\ell$ = the line area element.

Because of the symmetric property of $\underset{\sim}{\kappa}$, there is no contribution in the strain energy from the trace of $\underset{\sim}{\mu}$ on the left-hand side of Eq. 2-14.

To apply Eq. 2-14, the scalar product of $\delta\underset{\sim}{u}$ and Eq. 2-6 is formed and then integrated over the volume of B. By the divergence theorem,

$$\int_B \left(\tau_{ij}\ \delta\varepsilon_{ij} + \bar{\mu}_{ij}\ \delta\kappa_{ij}\right) dv = \int_{\partial B}\left[n_i\ \tau^S_{ij}\ \delta u_j + n_i\ \bar{\mu}_{ik}\ \delta w_k\right] ds \quad . \quad (2\text{-}15)$$

To convert the surface integral in Eq. 2-15 to the form of Eq. 2-14, the second integral can be written as

$$n_1 \bar{\mu}_{1k} \delta w_k = n_1 \mu_{1k} \left(\delta_{ki} - n_k n_i\right) \delta w_i + \frac{1}{2} e_{ijk} n_i \left(\mu_{nn} \delta u_k\right)_{,j}$$

$$- \frac{1}{2} e_{ijk} n_i \left(\mu_{nn,j} \delta u_k\right) \quad , \tag{2-16}$$

where

$$\bar{\mu}_{nn} = n_i n_j \bar{\mu}_{ij}$$

is a scalar function. Therefore, Eqs. 2-14 and 2-15, with the Stoke's theorem for the integral involving the last term of Eq. 2-16, yield

$$\int_{\partial B} \left(\bar{P}_i \delta u_i + \bar{Q}_i \delta w_i\right) ds + \int_C \bar{E}_i \delta u_i \, d\ell = \int_{\partial B} \Big[n_i \Big(\tau^S_{ik} - \frac{1}{2} e_{ijk} \bar{\mu}_{nn,j} \Big) \delta u_k + n_1 \bar{\mu}_{1k} \left(\delta_{ki} - n_k n_i\right) \delta w_i \Big] ds \tag{2-17}$$

$$+ \frac{1}{2} \int_C \left[\!\left[\bar{\mu}_{nn} \right]\!\right] t_k \delta u_k \, d\ell \quad ,$$

where $\underset{\sim}{t}$ = the unit tangent vector along the edge of the bounding surface, and

$[\![\ ]\!]$ = the difference of the quantity across the edge C.

By the standard argument of the calculus of variation, the traction boundary conditions for the stress and couple-stress fields are

$$\bar{P}_k = n_i \tau^S_{ik} + \frac{1}{2} e_{ijk} n_i \left(\bar{\mu}_{1j,1} - \bar{\mu}_{nn,j}\right) \quad ,$$

$$\bar{Q}_i = n_j \bar{\mu}_{jk} \left(\delta_{ki} - n_k n_i\right) \quad ,$$

$$\bar{E}_i = \frac{1}{2} t_i \left[\!\left[\bar{\mu}_{nn} \right]\!\right] \quad . \tag{2-18}$$

These boundary conditions, together with Eqs. 2-9, 2-10, and 2-12, complete the governing equations for the couple-stress theory of linear elasticity for homogeneous isotropic solids. In the following sections, the boundary value problem for the pure-bending of a circular cylinder is solved and compared with the classical beam theory.

3. PURE-BENDING OF CIRCULAR CYLINDER

It is convenient to adopt the circular cylindrical coordinate system r, θ, and z for the boundary value problems concerning the circular cylinders. The coordinate system for the circular cylinder under pure-bending was chosen so that the z-axis coincides with the central axis of the cylinder and the $\theta = 0$ direction (x-axis for the corresponding rectangular cartesian system) is perpendicular to the bending moment vector. The origin can be located at any point on the central axis.

Let ($\underset{\sim}{e}\langle r\rangle$, $\underset{\sim}{e}\langle\theta\rangle$, $\underset{\sim}{e}\langle z\rangle$) be the orthonormal basis at any point (r, θ, z) in the cylinder; then the displacement vector $\underset{\sim}{u}$ of this point has the vector representation

$$\underset{\sim}{u} = u_r \, \underset{\sim}{e}\langle r\rangle + u_\theta \, \underset{\sim}{e}\langle\theta\rangle + u_z \, \underset{\sim}{e}\langle z\rangle \quad , \tag{3-1}$$

where u_r, u_θ, and u_z = functions of r, θ, and z.

The governing equations in Section 2 can be converted to the cylindrical coordinate system by referring the partial derivatives as the covariant derivatives. Thus, the strain and rotation gradient tensors have the following components:

Strain Tensor Components

$$\varepsilon_{rr} = u_{r,r} \quad ,$$

$$\varepsilon_{\theta\theta} = \frac{1}{r} u_r + \frac{1}{r} u_{\theta,\theta} \quad ,$$

$$\varepsilon_{zz} = u_{z,z} \quad ,$$

$$\varepsilon_{r\theta} = \frac{1}{2}\left(u_{\theta,r} + \frac{1}{r}\,u_{r,\theta} - \frac{1}{r}\,u_{\theta}\right) \quad , \tag{3-2}$$

$$\varepsilon_{rz} = \frac{1}{2}\left(u_{z,r} + u_{r,z}\right) \quad ,$$

$$\varepsilon_{\theta z} = \frac{1}{2}\left(u_{\theta,z} + \frac{1}{r}\,u_{z,\theta}\right) \quad ,$$

Rotation Gradient Tensor Components

$$\kappa_{rr} = \frac{1}{2}\left(\frac{1}{r}\,u_{z,\theta r} - \frac{1}{r^2}\,u_{z,\theta} - u_{\theta,rz}\right) \quad ,$$

$$\kappa_{\theta\theta} = \frac{1}{2}\left(\frac{1}{r}\,u_{r,\theta z} - \frac{1}{r}\,u_{z,r\theta} + \frac{1}{r^2}\,u_{z,\theta} - \frac{1}{r}\,u_{\theta,z}\right) \quad ,$$

$$\kappa_{zz} = \frac{1}{2}\left(u_{\theta,rz} + \frac{1}{r}\,u_{\theta,z} - \frac{1}{r}\,u_{r,\theta z}\right) \quad ,$$

$$\kappa_{r\theta} = \frac{1}{2}\left(u_{r,rz} - u_{z,rr}\right) \quad ,$$

$$\kappa_{\theta r} = \frac{1}{2}\left(\frac{1}{r^2}\,u_{z,\theta\theta} - \frac{1}{r}\,u_{\theta,\theta z} - \frac{1}{r}\,u_{r,z} + \frac{1}{r}\,u_{z,r}\right) \quad , \tag{3-3}$$

$$\kappa_{rz} = \frac{1}{2}\left(u_{\theta,rr} + \frac{1}{r}\,u_{\theta,r} - \frac{1}{r}\,u_{r,r\theta} + \frac{1}{r^2}\,u_{r,\theta} - \frac{1}{r^2}\,u_{\theta}\right) \quad ,$$

$$\kappa_{zr} = \frac{1}{2}\left(\frac{1}{r}\,u_{z,z\theta} - u_{\theta,zz}\right) \quad ,$$

$$\kappa_{\theta z} = \frac{1}{2}\left(\frac{1}{r}\,u_{\theta,r\theta} + \frac{1}{r^2}\,u_{\theta,\theta} - \frac{1}{r^2}\,u_{r,\theta\theta}\right) \quad ,$$

$$\kappa_{z\theta} = \frac{1}{2}\left(u_{r,zz} - u_{z,rz}\right) \quad .$$

In Eqs. 3-2 and 3-3 and in what follows, $(\ )_{,r}$ stands for the partial derivatives with respect to r, etc. The stress tensor and couple-stress tensor are a straightforward substitution of Eqs. 3-2 and 3-3 into Eq. 2-10.

For the boundary condition Eq. 2-17 on the cylinder surface, $\bar{\mu}_{\ell j,\ell}$ is the divergence of $\underset{\sim}{\bar{\mu}}$, and the unit normal to the bounding surface of a circular cylinder is $\underset{\sim}{n} = \underset{\sim}{e}_{<r>}$. Thus, $\bar{\mu}_{nn} = \bar{\mu}_{rr}$ and the boundary conditions for the cylinder become

$$
\begin{aligned}
\bar{P}_r &= \tau^S_{rr} \quad , \\
\bar{P}_\theta &= \tau^S_{r\theta} + \frac{1}{2}\bar{\mu}_{rr,z} - \frac{1}{2}\left(\bar{\mu}_{rz,r} + \frac{1}{r}\bar{\mu}_{\theta z,\theta} + \bar{\mu}_{zz,z} + \frac{1}{r}\bar{\mu}_{rz}\right) \quad , \\
\bar{P}_z &= \tau^S_{rz} - \frac{1}{2r}\bar{\mu}_{rr,\theta} + \frac{1}{2}\left(\bar{\mu}_{r\theta,r} + \frac{1}{r}\bar{\mu}_{\theta\theta,\theta} + \bar{\mu}_{z\theta,z}\right. \\
&\quad \left. + \frac{1}{r}\bar{\mu}_{r\theta} + \frac{1}{r}\bar{\mu}_{\theta r}\right) \quad , \qquad (3\text{-}4) \\
\bar{Q}_\theta &= \bar{\mu}_{r\theta} \quad , \\
\bar{Q}_z &= \bar{\mu}_{rz} \quad ,
\end{aligned}
$$

with no edge on the surface for an infinite cylinder, $\underset{\sim}{\bar{E}} = 0$.

The classical linear elastic solution of the pure-bending of a circular cylinder is studied next. Since the circular cylinder is a special case of the prismatic bar whose solution can be found in most texts of elasticity (e.g., Ref. 5), disregarding the rigid body of motions, this solution is recorded in circular cylindrical coordinate system as follows:

$$
\begin{aligned}
u_r &= -\frac{1}{2}\left(\nu r^2 + z^2\right)\frac{\cos\theta}{\rho} \quad , \\
u_\theta &= -\frac{1}{2}\left(\nu r^2 - z^2\right)\frac{\sin\theta}{\rho} \quad , \qquad (3\text{-}5)
\end{aligned}
$$

$$u_z = zr \frac{\cos\theta}{\rho} \quad ,$$

where ρ = the radius of curvature of the bent cylinder, and

ν = the Poisson's ratio.

Lamé constants λ and μ can be related to Young's modulus E and Poisson's ratio ν by

$$\lambda = \frac{\nu E}{(1+\nu)(1-2\nu)} \quad , \quad \mu = \frac{E}{2(1+\nu)} \quad . \tag{3-6}$$

Since the displacement vector function given by Eq. 3-5 satisfies the Laplace equation for the equilibrium of the elastic media in classical theory, Eq. 2-12 is also satisfied. Therefore, if $\underset{\sim}{u}$ is a solution for the couple-stress theory, it has to satisfy the traction-free boundary conditions.

As has been computed in Ref. 5, the symmetric stress tensor $\underset{\sim}{\tau}^S$ has the components

$$\tau^S_{zz} = \frac{Er}{\rho}\cos\theta \quad ,$$

$$\tau^S_{rr} = \tau^S_{\theta\theta} = \tau^S_{r\theta} = \tau^S_{\theta z} = \tau^S_{rz} = 0 \quad . \tag{3-7}$$

The couple-stress is calculated from Eqs. 3-5, 3-3, and 2-10b:

$$\bar{\mu}_{rz} = -4\left(\nu\bar{d}_1 + \bar{d}_2\right)\frac{\sin\theta}{\rho} \quad ,$$

$$\bar{\mu}_{zr} = -4\left(\bar{d}_1 + \nu\bar{d}_2\right)\frac{\sin\theta}{\rho} \quad ,$$

$$\bar{\mu}_{\theta z} = -4\left(\nu d_1 + d_2\right)\frac{\cos\theta}{\rho} \quad , \tag{3-8}$$

$$\bar{\mu}_{z\theta} = -4\left(\bar{d}_1 + \nu\bar{d}_2\right)\frac{\cos\theta}{\rho} \quad ,$$

$$\bar{\mu}_{rr} = \bar{\mu}_{\theta\theta} = \bar{\mu}_{zz} = \bar{\mu}_{r\theta} = \bar{\mu}_{\theta r} = 0 \quad .$$

Substituting Eqs. 3-7 and 3-8 into Eq. 3-4, one finds that the traction-free boundary conditions are not satisfied for the surface couple $\bar{Q}_z$:

$$\bar{Q}_z = -4\left(\nu\bar{d}_1 + \bar{d}_2\right)\frac{\sin\theta}{\rho} \quad , \tag{3-9}$$

but the rest of the free traction boundary conditions are satisfied. In other words, Eq. 3-5 is a solution of the couple-stress theory for a circular cylinder only if a distributed surface couple $\bar{Q}_z$ given by Eq. 3-9 is applied.

Since it is assumed that there is no surface couple nor surface force applied on the cylinder surface, the classical elastic solution (Eq. 3-5) is not a solution of the pure-bending of the circular cylinder in the couple-stress theory. To construct a solution for this problem, a secondary deformation field $\underset{\sim}{u}^{(1)}$, which satisfied Eq. 2-12 and the traction boundary conditions, is introduced:

$$\begin{aligned} &\bar{P}_r = \bar{P}_\theta = \bar{P}_z = \bar{Q}_\theta = 0 \quad , \\ &\bar{Q}_z = 4\left(\nu\bar{d}_1 + \bar{d}_2\right)\frac{\sin\theta}{\rho} \quad , \qquad \text{at } r = z \quad . \end{aligned} \tag{3-10}$$

Consequently, the superposition $\underset{\sim}{u} + \underset{\sim}{u}^{(1)}$ will satisfy the free traction boundary conditions and Eq. 2-12. Since the boundary condition (Eq. 3-10) is uniform along the cylinder, the boundary value problem for $\underset{\sim}{u}^{(1)}$ can be regarded as a plane-strain problem. The next section is devoted to solving this plane-strain problem.

4. SOLUTION OF THE PLANE STRAIN PROBLEM

The displacement of $\underset{\sim}{u}^{(1)}$ of the plane-strain problem that was deduced in Section 3 is solved here. For simplicity, the superscript in $\underset{\sim}{u}^{(1)}$ is deleted in this section. In the cylindrical coordinate system, the plane strain displacement $\underset{\sim}{u}$ has the general representation

$$\underset{\sim}{u} = u_r\,(r,\theta)\ \underset{\sim}{e}\langle r\rangle + u_\theta\,(r,\theta)\ \underset{\sim}{e}\langle\theta\rangle \quad , \tag{4-1}$$

where u_r and u_θ are sufficiently continuously differentiable scalar valued functions of r and θ.

In solving for $\underset{\sim}{u}$, the divergence and curl operations, respectively, are applied to Eq. 2-12 to yield the following pair of partial differential equations:

$$\begin{aligned} &\nabla^2\ \nabla\cdot\underset{\sim}{u} = 0 \quad , \\ &(1 - \ell_2^2\ \nabla^2)\ \nabla^2\ (\nabla \times \underset{\sim}{u}) = 0 \quad . \end{aligned} \tag{4-2}$$

According to the boundary conditions (Eq. 3-10) for Eq. 4-2, a solution that is a linear function of sin θ and cos θ is expected. Thus,

$$\begin{aligned} u_r = &\left[-C_2\ \ell_2^2\ \frac{\ell_2}{r}\ I_1\left(\frac{r}{\ell_2}\right) - D_2\ \ell_2^3\ \frac{\ell_2}{r}\ K_1\left(\frac{r}{\ell_2}\right) + E_1\ r^2 + F_1\ \ell nr\right. \\ &\left. + G_1\ r^{-2} - H_1\right]\ \cos\theta + \left[A_2\ \ell_2^3\ \frac{\ell_2}{r}\ I_1\left(\frac{r}{\ell_2}\right) + B_2\ \ell_2^3\ \frac{\ell_2}{r}\ K_1\left(\frac{r}{\ell_2}\right)\right. \\ &\left. + E_2\ r^2 + F_2\ \ell nr - G_2\ r^{-2} + H_2\right]\ \sin\theta \quad , \end{aligned}$$

$$u_\theta = \left[C_2 \ell_2^3 \left\{ I_0\left(\frac{r}{\ell_2}\right) - \frac{\ell_2}{r} I_1\left(\frac{r}{\ell_2}\right) \right\} - D_2 \ell_2^3 \left\{ K_0\left(\frac{r}{\ell_2}\right) + \frac{\ell_2}{r} K_1\left(\frac{r}{\ell_2}\right) \right\} \right. \tag{4-3}$$

$$\left. + E_3 r^2 + F_3 \ell nr + G_1 r^{-2} + H_1 \right] \sin\theta + \left[A_2 \ell_2^3 \left\{ I_0\left(\frac{r}{\ell_2}\right) \right.\right.$$

$$\left.\left. - \frac{\ell_2}{r} I_1\left(\frac{r}{\ell_2}\right) \right\} - B_2 \ell_2^3 \left\{ K_0\left(\frac{r}{\ell_2}\right) + \frac{\ell_2}{r} K_1\left(\frac{r}{\ell_2}\right) \right\} + E_4 r^2 + F_4 \ell nr \right.$$

$$\left. + G_2 r^{-2} + H_2 \right] \cos\theta \quad ,$$

where $I_n(\ )$ and $K_n(\ )$ = the modified Bessel functions of the first and second kinds, respectively, n equals 0, 1, (Ref. 6), and

A_2, B_2, ... = constants of integration.

The requirement of the continuous differentiability of u_r and u_θ means that, for a simply connected cylinder, the integration constants must satisfy

$$B_2 = D_2 = F_1 = F_2 = F_3 = F_4 = G_1 = G_2 = 0 \quad ,$$

$$H_1 = -\frac{1}{2} C_2 \ell_2^3 \quad , \tag{4-4}$$

$$H_2 = -\frac{1}{2} A_2 \ell_2^3 \quad .$$

The solution (Eq. 4-3) for a simply connected cylinder is therefore simplified to

$$u_r = \left[A_2 \frac{\ell_2^4}{r} I_1\left(\frac{r}{\ell_2}\right) + E_2 r^2 - \frac{1}{2} A_2 \ell_2^3 \right] \sin\theta - \left[C_2 \frac{\ell_2^4}{r} I_1\left(\frac{r}{\ell_2}\right) \right.$$

$$\left. - E_1 r^2 - \frac{1}{2} C_2 \ell_2^3 \right] \cos\theta \quad , \tag{4-5}$$

$$u_\theta = \left[C_2\, \ell_2^3 \left\{ I_0\left(\frac{r}{\ell_2}\right) - \frac{\ell_2}{r}\, I_1\left(\frac{r}{\ell_2}\right)\right\} + E_3\, r^2 - \frac{1}{2}\, C_2\, \ell_2^3\right] \sin\theta$$

$$+ \left[A_2\, \ell_2^3 \left\{ I_0\left(\frac{r}{\ell_2}\right) - \frac{\ell_2}{r}\, I_1\left(\frac{r}{\ell_2}\right)\right\} + E_4\, r^2 - \frac{1}{2}\, A_2\, \ell_2^3\right] \cos\theta \quad , \tag{4-5}$$

where A_2, C_2, E_1, E_2, E_3, and E_4 = constants to be determined by the boundary conditions.

To apply Eq. 3-10, it will be convenient here to express $\underset{\sim}{\bar{P}}$ and $\underset{\sim}{\bar{Q}}$ in terms of $\underset{\sim}{u}$ of Eqs. 4-1 and 4-5. Using Eqs. 2-10, 3-2, 3-3, and 3-4, the boundary conditions become

$$\lambda\left(u_{r,r} + \frac{1}{r}\, u_r + \frac{1}{r}\, u_{\theta,\theta}\right) + 2\mu\, u_{r,r}\Big|_{r=a} = 0 \quad , \tag{4-6a}$$

$$\mu\left(u_{\theta,r} + \frac{1}{r}\, u_{r,\theta} - \frac{1}{r}\, u_\theta\right) - \bar{d}_1\left(-\frac{1}{r}\, u_{r,rr\theta} + u_{\theta,rrr} + \frac{1}{r^2}\, u_{\theta,\theta\theta r}\right.$$

$$\left. - \frac{1}{r^3}\, u_{r,\theta\theta\theta} + \frac{1}{r^2}\, u_{r,r\theta} + \frac{2}{r}\, u_{\theta,rr} + \frac{1}{r^3}\, u_{\theta,\theta\theta}\right. \tag{4-6b}$$

$$\left. - \frac{1}{r^3}\, u_{r,\theta} - \frac{1}{r^2}\, u_{\theta,r} + \frac{1}{r^3}\, u_\theta\right)\Big|_{r=a} = 0 \quad ,$$

$$2\bar{d}_1\left(u_{\theta,rr} + \frac{1}{r}\, u_{\theta,r} - \frac{1}{r^2}\, u_\theta - \frac{1}{r}\, u_{r,r\theta} + \frac{1}{r^2}\, u_{r,\theta}\right)\Big|_{r=a} \tag{4-6c}$$

$$= 4\, \frac{\nu\bar{d}_1 + \bar{d}_2}{\rho} \sin\theta \quad ,$$

where a = the radius of the cylindrical beam.

Substituting Eq. 4-5 into Eq. 4-6, since sin θ and cos θ are linearly independent, obtains

$$A_2 = E_2 = E_4 = 0 \quad . \tag{4-7}$$

The remaining integration constants are solved from Eq. 4-6.

$$C_2 = \frac{\left(\nu + \frac{\bar{d}_2}{\bar{d}_1}\right)\Big/\rho\ell_2}{\left[\frac{1}{2} + 4(1-\nu)\frac{\ell_2^2}{a^2}\right] I_0\left(\frac{a}{\ell_2}\right) - \left[\frac{1}{2}\frac{\ell_2}{a} + 8(1-\nu)\frac{\ell_2^3}{a^3}\right] I_1\left(\frac{a}{\ell_2}\right)} \quad ,$$

$$E_1 = \frac{\left[(1-4\nu)\left(\nu + \frac{\bar{d}_2}{\bar{d}_1}\right)\Big/\rho\right] \cdot \frac{\ell_2^2}{a^2}\left[\frac{1}{2} I_0\left(\frac{a}{\ell_2}\right) - \frac{\ell_2}{a} I_1\left(\frac{a}{\ell_2}\right)\right]}{\left[\frac{1}{2} + 4(1-\nu)\frac{\ell_2^2}{a^2}\right] I_0\left(\frac{a}{\ell_2}\right) - \left[\frac{1}{2}\frac{\ell_2}{a} + 8(1-\nu)\frac{\ell_2^3}{a^3}\right] I_1\left(\frac{a}{\ell_2}\right)} \quad , \tag{4-8}$$

$$E_3 = \frac{\left[(5-4\nu)\left(\nu + \frac{\bar{d}_2}{\bar{d}_1}\right)\Big/\rho\right] \cdot \frac{\ell_2^2}{a^2}\left[\frac{1}{2} I_0\left(\frac{a}{\ell_2}\right) - \frac{\ell_2}{a} I_1\left(\frac{a}{\ell_2}\right)\right]}{\left[\frac{1}{2} 4(1-\nu)\frac{\ell_2^2}{a^2}\right] I_0\left(\frac{a}{\ell_2}\right) - \left[\frac{1}{2}\frac{\ell_2}{a} + 8(1-\nu)\frac{\ell_2^3}{a^3}\right] I_1\left(\frac{a}{\ell_2}\right)} \quad ,$$

where the Lamé constants λ and μ are replaced by the Young's modulus E and Poisson's ratio ν through Eq. 3-6.

5. BENDING MOMENT AND STRESS

The displacement field of the circular cylinder with couple-stresses under pure bending is the superposition of Eq. 4-5 to the classical linear elastic solution (Eq. 3-5). The stress and couple-stress tensors can therefore be calculated from the kinematic equations (Eqs. 3-2 and 3-3), the constitutive relations (Eq. 2-10), and the stress equation (Eq. 2-8). The bending moment-curvature relation can also be obtained.

From the equation of equilibrium (Eq. 2-1b), the bending moment in the couple-stress theory is computed by the formula

$$\underset{\sim}{M} = \int_A [\underset{\sim}{r} \times (\underset{\sim}{n}\,\underset{\sim}{\tau}) + \underset{\sim}{n}\,\underset{\sim}{\mu}]\, ds \quad , \tag{5-1}$$

where $\underset{\sim}{M}$ = the bending moment vector,

A = the cross section,

$\underset{\sim}{n}$ = the unit normal to the area element ds, and

$\underset{\sim}{r}$ = the position vector.

The explicit expansion of this formula in the cylindrical coordinate system for a cross section perpendicular to z-axis is

$$M_x = \int_o \int_0^{2\pi} \left[r \sin\theta\, \tau_{zz} + \mu_{zr} \cos\theta - \mu_{z\theta} \sin\theta \right] r\, dr\, d\theta \quad ,$$

$$M_y = \int_o \int_0^{2\pi} \left[-r \cos\theta\, \tau_{zz} + \mu_{zr} \sin\theta + \mu_{z\theta} \cos\theta \right] r\, dr\, d\theta \quad , \tag{5-2}$$

where M_x and M_y = the components of the bending moment about the x-axis and y-axis, respectively.

Since the stress and couple-stress components due to the displacement $\underset{\sim}{u}$ of Eq. 3-5 are given by Eqs. 3-7 and 3-8, respectively, only the stress and couple-stress fields due to the displacement $\underset{\sim}{u}^{(1)}$ given by Eq. 4-5 need further elaboration. Substitutions of Eq. 4-5 into Eqs. 3-2 and 3-3 yield the following components of $\underset{\sim}{\varepsilon}^{(1)}$ and $\underset{\sim}{\kappa}^{(1)}$:

Strain Tensor Components

$$\varepsilon_{rr}^{(1)} = \left\{ C_2 \ell_2^2 \left[- \frac{\ell_2}{r} I_0 \left(\frac{r}{\ell_2} \right) + 2 \frac{\ell_2^2}{r^2} I_1 \left(\frac{r}{\ell_2} \right) \right] + 2 E_1 r \right\} \cos \theta \quad ,$$

$$\varepsilon_{\theta\theta}^{(1)} = \left\{ C_2 \ell_2^2 \left[\frac{\ell_2}{r} I_0 \left(\frac{r}{\ell_2} \right) - 2 \frac{\ell_2^2}{r^2} I_1 \left(\frac{r}{\ell_2} \right) \right] + \left(E_1 + E_3 \right) r \right\} \cos \theta \quad ,$$

$$\varepsilon_{r\theta}^{(1)} = \left\{ C_2 \ell_2^2 \left[- \frac{\ell_2}{r} I_0 \left(\frac{r}{\ell_2} \right) + \left(\frac{1}{2} + 2 \frac{\ell_2^2}{r^2} \right) I_1 \left(\frac{r}{\ell_2} \right) \right] \right.$$

$$\left. - \frac{1}{2} \left(E_1 - E_3 \right) r \right\} \sin \theta \quad ,$$

$$\varepsilon_{zz}^{(1)} = \varepsilon_{zr}^{(1)} = \varepsilon_{z\theta}^{(1)} = 0 \quad , \qquad (5\text{-}3)$$

Rotation Gradient Components

$$\kappa_{rz}^{(1)} = \left\{ \frac{1}{2} C_2 \ell_2 \left[I_0 \left(\frac{r}{\ell_2} \right) - \frac{\ell_2}{r} I_1 \left(\frac{r}{\ell_2} \right) \right] + \frac{1}{2} \left(E_1 + 3E_3 \right) \right\} \sin \theta \quad ,$$

$$\kappa_{\theta z}^{(1)} = \left\{ \frac{1}{2} C_2 \ell_2 \frac{\ell_2}{r} I_1 \left(\frac{r}{\ell_2} \right) + \frac{1}{2} \left(E_1 + 3E_3 \right) \right\} \cos \theta \quad ,$$

$$\kappa_{zr}^{(1)} = \kappa_{z\theta}^{(1)} = \kappa_{r\theta}^{(1)} = \kappa_{rr}^{(1)} = \kappa_{\theta\theta}^{(1)} = \kappa_{zz}^{(1)} = 0 \quad .$$

Eqs. 5-3 and 2-10 then yield $\underset{\sim}{\tau}^{S(1)}$ and $\underset{\sim}{\bar{\mu}}^{(1)}$. These results are superposed to Eqs. 3-7 and 3-8, respectively, then Eq. 2-8 is employed to obtain the stress tensor $\underset{\sim}{\tau}$:

$$\tau_{rr} = \lambda \left(3E_1 + E_3\right) r \cos\theta + 2\mu \left\{C_2 \ell_2^2 \left[-\frac{\ell_2}{r} I_0\left(\frac{r}{\ell_2}\right) + 2\frac{\ell_2^2}{r^2} I_1\left(\frac{r}{\ell_2}\right)\right] + 2E_1 r\right\} \cos\theta \quad ,$$

$$\tau_{\theta\theta} = \lambda \left(3E_1 + E_3\right) r \cos\theta + 2\mu \left\{C_2 \ell_2^2 \left[\frac{\ell_2}{r} I_0\left(\frac{r}{\ell_2}\right) - 2\frac{\ell_2^2}{r^2} I_1\left(\frac{r}{\ell_2}\right)\right] + \left(E_1 + E_3\right) r\right\} \cos\theta \quad , \qquad (5\text{-}4a)$$

$$\tau_{zz} = \left[\frac{E}{\rho} + \lambda \left(3E_1 + E_3\right)\right] r \cos\theta \quad ,$$

$$\tau_{r\theta} = -C_2 \bar{d}_1 I_1\left(\frac{r}{\ell_2}\right) \sin\theta = -\tau_{\theta r} \quad ,$$

$$\tau_{r\theta} = \tau_{\theta z} = \tau_{zr} = \tau_{z\theta} = 0 \quad .$$

The couple-stresses are

$$\bar{\mu}_{rz} = -4\left(\nu\bar{d}_1 + \bar{d}_2\right)\frac{\sin\theta}{\rho} + 2\bar{d}_1\left\{C_2\,\ell_2\left[I_0\left(\frac{r}{\ell_2}\right) - \frac{\ell_2}{r}I_1\left(\frac{r}{\ell_2}\right)\right] + \left(E_1 + 3E_3\right)\right\}\sin\theta \quad .$$

$$\bar{\mu}_{zr} = -4\left(\bar{d}_1 + \nu\bar{d}_2\right)\frac{\sin\theta}{\rho} + 2\bar{d}_2\left\{C_2\,\ell_2\left[I_0\left(\frac{r}{\ell_2}\right) - \frac{\ell_2}{r}I_1\left(\frac{r}{\ell_2}\right)\right] + \left(E_1 + 3E_3\right)\right\}\sin\theta \quad ,$$

$$\bar{\mu}_{\theta z} = -4\left(\nu\bar{d}_1 + \bar{d}_2\right)\frac{\cos\theta}{\rho} + 2\bar{d}_1\left\{C_2\,\ell_2\,\frac{\ell_2}{r}I_1\left(\frac{r}{\ell_2}\right) + \left(E_1 + 3E_3\right)\right\}\cos\theta \quad , \qquad (5\text{-}4b)$$

$$\bar{\mu}_{z\theta} = -4\left(\bar{d}_1 + \nu\bar{d}_2\right)\frac{\cos\theta}{\rho} + 2\bar{d}_2\left\{C_2\,\ell_2\,\frac{\ell_2}{r}I_1\left(\frac{r}{\ell_2}\right) + \left(E_1 + 3E_3\right)\right\}\cos\theta \quad ,$$

$$\bar{\mu}_{rr} = \bar{\mu}_{\theta\theta} = \bar{\mu}_{zz} = \bar{\mu}_{r\theta} = \bar{\mu}_{\theta r} = 0 \quad ,$$

where the Lamé constants λ and μ in the stress tensor are related to E and ν by Eq. 3-6. Using Eq. 5-2, the bending moment is obtained:

$$M_x = 0 \quad . \qquad (5\text{-}4c)$$

$$M_y = -I_y \left[\frac{E}{\rho} + \frac{16}{\rho a^2} \left(\bar{d}_1 + \nu \bar{d}_2 \right) + \frac{\nu E}{(1+\nu)(1-2\nu)} \left(3E_1 + E_3 \right) \right.$$
$$\left. - \frac{8\bar{d}_2}{a^2} \left(E_1 + 3E_3 \right) - 8\bar{d}_2 \frac{C_2 \ell_2^2}{a^3} I_1 \left(\frac{a}{\ell_2} \right) \right] \quad , \tag{5-5}$$

where $I_y = \pi a^4/4$ is the area moment of inertia with respect to the y-axis. Using C_2, E_1, and E_2 given by Eq. 4-8,

$$M_y = -\frac{EI_y}{\rho} C_m \quad ,$$

$$C_m = 1 + \frac{8 \frac{\ell_2^2}{a^2}}{1+\nu} \cdot \left\{ \frac{1}{2} \left(1 - \frac{\bar{d}_2^2}{\bar{d}_1^2} \right) \frac{\ell_2}{a} I_1 \left(\frac{a}{\ell_2} \right) + \left[\frac{1}{2} I_0 \left(\frac{a}{\ell_2} \right) \right. \right.$$
$$\left. \left. - \frac{\ell_2}{a} I_1 \left(\frac{a}{\ell_2} \right) \right] \left[1 + \nu^2 + 2\nu \frac{\bar{d}_2}{\bar{d}_1} + 8(1-\nu) \left(1 - \frac{\bar{d}_2^2}{\bar{d}_1^2} \right) \frac{\ell_2^2}{a^2} \right] \right\} \tag{5-6}$$
$$\cdot \left\{ \left[\frac{1}{2} + 4(1-\nu) \frac{\ell_2^2}{a^2} \right] I_0 \left(\frac{a}{\ell_2} \right) - \left[\frac{1}{2} + 8(1-\nu) \frac{\ell_2^2}{a^2} \right] \right.$$
$$\left. \frac{\ell_2}{a} I_1 \left(\frac{a}{\ell_2} \right) \right\}^{-1} \quad ,$$

where C_m = the coefficient of bending moment for the pure-bending of a circular cylinder, or simply moment coefficient. From Eq. 5-4c,

$$\tau_{zz} = C_t E \frac{r \cos \theta}{\rho} \quad ,$$

$$C_t = 1 + \frac{8\frac{\ell_2^2}{a^2}}{1+\nu} \cdot \frac{\nu\left(\nu + \frac{\bar{d}_2}{\bar{d}_1}\right)\left[\frac{1}{2} I_0\left(\frac{a}{\ell_2}\right) - \frac{\ell_2}{a} I_1\left(\frac{a}{\ell_2}\right)\right]}{\left[\frac{1}{2} + 4(1-\nu)\frac{\ell_2^2}{a^2}\right] I_0\left(\frac{a}{\ell_2}\right) - \left[\frac{1}{2}\frac{\ell_2}{a} + 8(1-\nu)\frac{\ell_2^3}{a^3}\right] I_1\left(\frac{a}{\ell_2}\right)}, \quad (5\text{-}7)$$

(5-7)

where C_t = the coefficient of axial flexural stress for the pure-bending of a circular cylinder, or simply the stress coefficient. Both C_m and C_t are dependent on the geometry (radius a), as well as the material property (ν, $\bar{d}_1$, and $\bar{d}_2$). Also, C_t is a linear function of $\bar{d}_2$, but C_m is a quadratic function of $\bar{d}_2$.

The numerical values of C_m and C_t with $\bar{d}_2/\bar{d}_1$ as a parameter are plotted in Figs. 5-1 through 5-3 for ν = 0.1, 0.15, and 0.2, respectively. From these results, the negligence of the couple-stresses in the analysis will yield errors of less than 10% for both bending moment and axial fluexural stress if $a/\ell_2 > 10$.

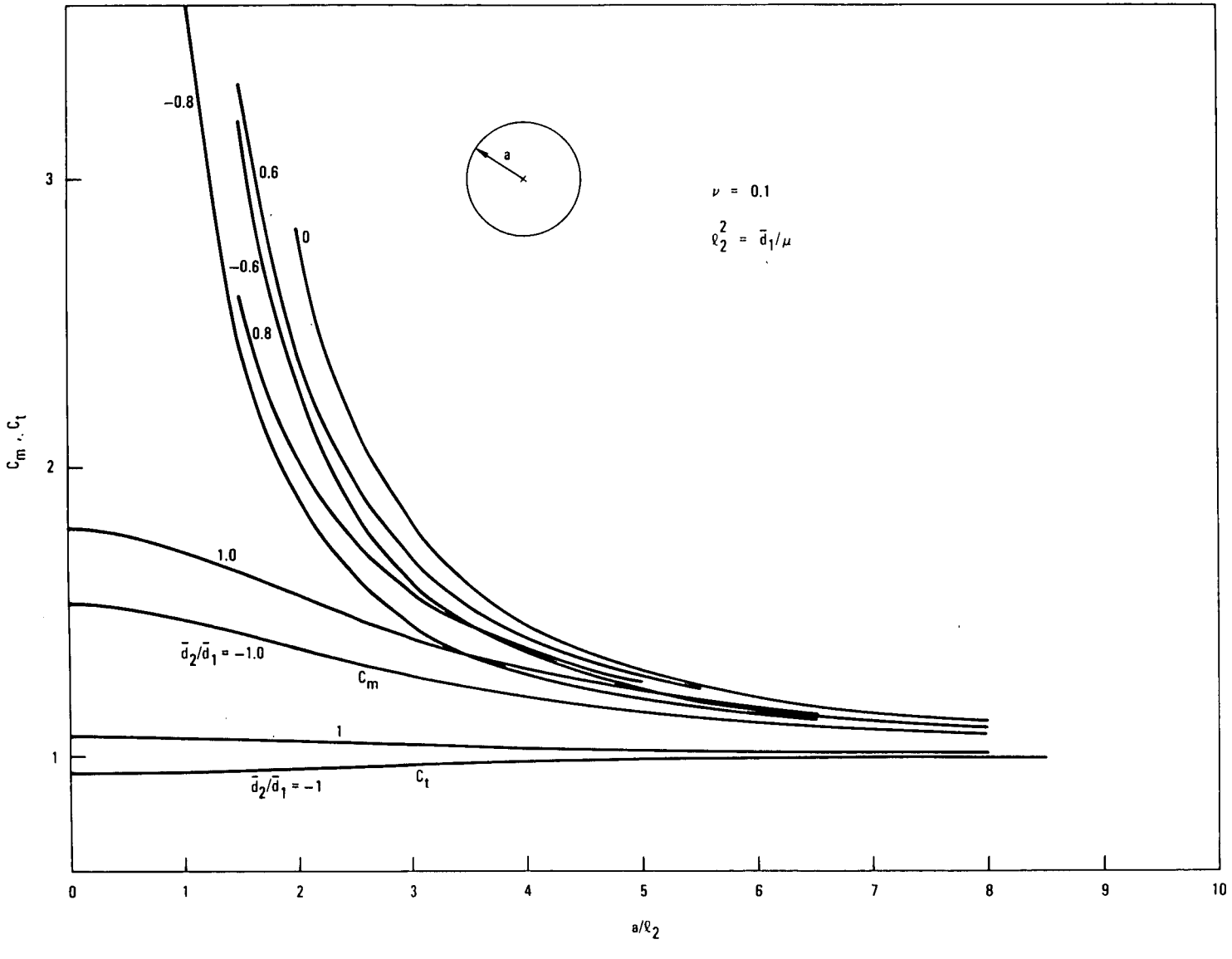

Fig. 5-1. Coefficient of bending moment C_m and axial flexural stress C_t for Poisson's ratio $\nu = 0.1$

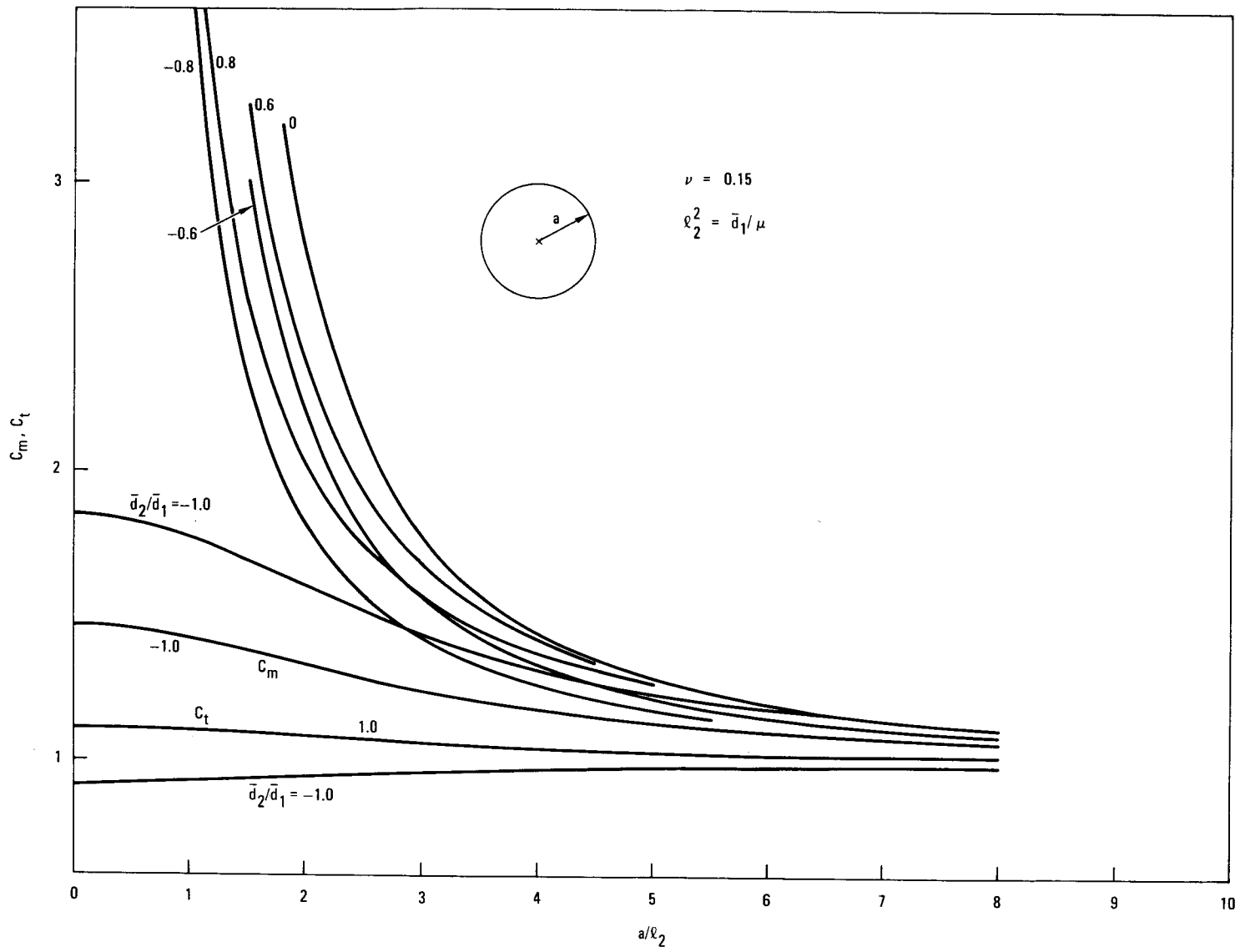

Fig. 5-2. Coefficient of bending moment C_m and axial flexural stress C_t for Poisson's ratio $\nu = 0.15$

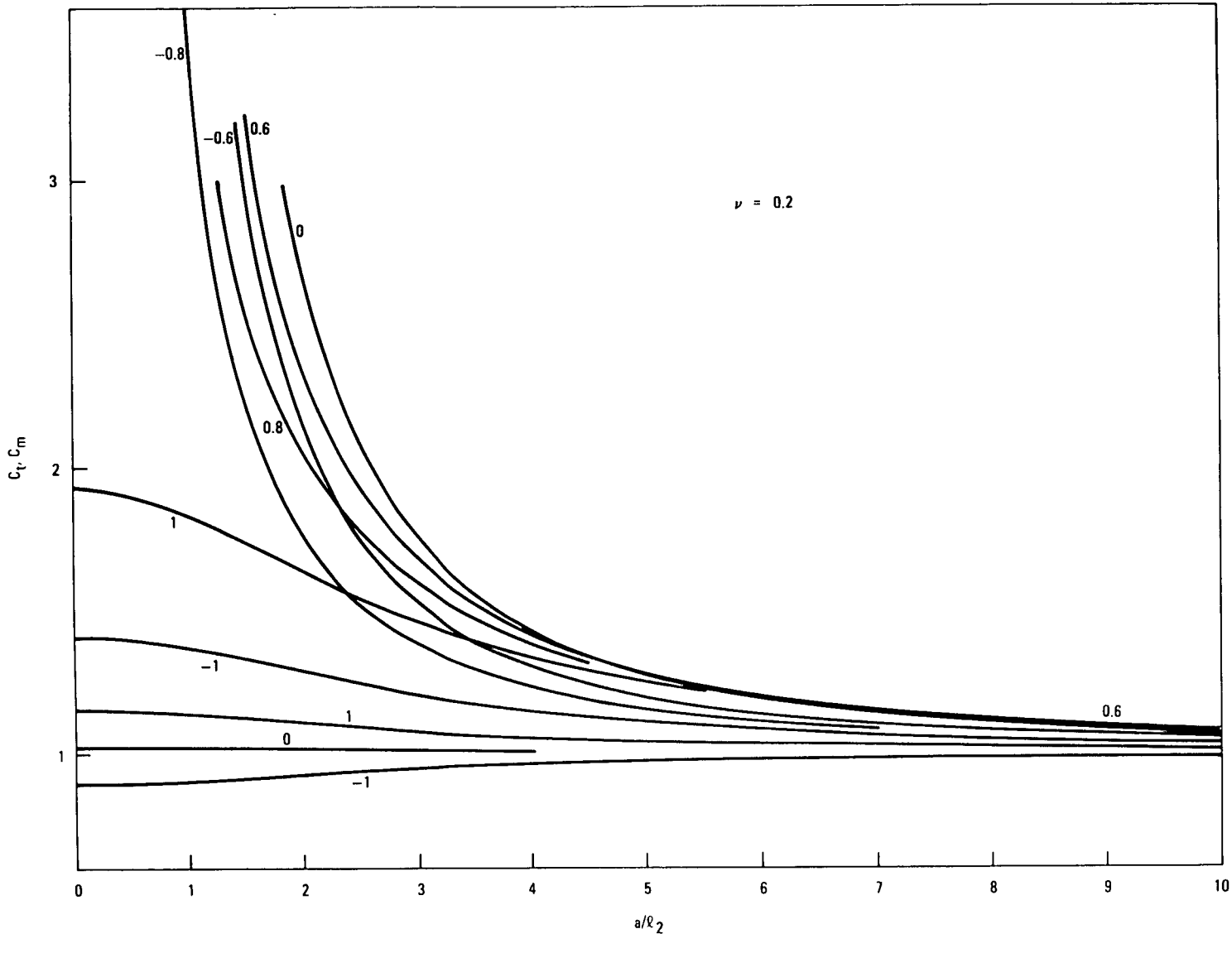

Fig. 5-3. Coefficient of bending moment C_m and axial flexural stress C_t for Poisson's ratio $\nu = 0.2$

6. SUMMARY OF THE COUPLE-STRESS SOLUTION

To facilitate comparing couple-stress theory and the classical elasticity theory, some aspects of the results of previous sections are summarized below:

1. The couple-stresses cause an in-plane deformation (Eq. 4-5) in addition to the classical elastic deformation (Eq. 3-5), and the stress (in Eq. 5-4) is not uniaxially aligned along the beam axis as in the classical beam theory.

2. The axial stress τ_{zz} and the bending moment M_y are proportional to Ex/ρ ($x = r \cos\theta$) and EI_y/ρ, Eqs. 5-7 and 5-6, respectively. The proportional coefficients, stress coefficient C_t and moment coefficient C_m, are functions of the cylinder cross section (radius a) and the material constants but independent of the bending curvature.

3. The axial stress coefficient C_t is a linear function of $\bar{d}_2$ and has the following properties:

$$C_t \gtreqless 1 \qquad \text{if } \nu\left(\nu + \frac{\bar{d}_2}{\bar{d}_1}\right) \gtreqless 0 \quad , \tag{6-1}$$

$$C_t \to 1 \qquad \text{as } a \to \infty \quad , \tag{6-2}$$

and

$$C_t = 1 + 0(\nu) \quad \text{if } |\nu| \text{ is small} \quad . \tag{6-3}$$

4. The bending moment coefficient C_m is a quadratic function of $\bar{d}_2$ and decreases with the increase of the radius a for a given material. It also has the following properties:

$$C_m > 1 \quad , \tag{6-4}$$

$$C_m \to 1 \qquad \text{as } a \to \infty \quad , \tag{6-5}$$

and

$$C_m \to 8 \frac{1 - \left(\frac{\bar{d}_2}{\bar{d}_1}\right)^2}{1 - \nu} \frac{\ell_2^2}{a^2} \qquad \text{as } a \to 0 \quad . \tag{6-6}$$

5. The bending moment coefficient C_m is always greater than the axial stress coefficient C_t.

6. From the numerical values of C_m and C_t shown in Figs. 5-1 to 5-3, it is concluded that for Posson's ratio $\nu \tilde{\sim} 0.1$; the negligence of the couple-stresses in the pure-bending of the circular cylinder will yield errors of less than 10% in axial stress and bending moment, respectively, if a/ℓ_2 is greater than 10.

7. APPLICATION TO THE GRAPHITE

From the characteristics of C_m and C_t as given in Section 6 and shown in Figs. 5-1 through 5-3, it is seen that C_t is fairly close to 1 for small $|\nu|$, but C_m varies considerably in the midrange of a/ℓ_2. Moreover, C_m can be easily determined experimentally by using Eq. 5-6 for a given circular cylinder. These properties make the measured C_m a favorable choice for the purpose of identifying the influence of the couple-stresses in a given material. Other relevant facts shall also be examined subsequently to fully confirm that the observed mechanical responses are caused by the presence of couple-stresses. This section compares experimentally measured data of pure-bending with theoretical implications to show how couple-stresses influence observed graphite phenomena.

Recent literature contains a considerable amount of experimental data concerning graphite mechanical behavior. Most of these experiments, however, are designed according to the classical elasticity; hence, the data primarily display the inconsistency of the classical elasticity in characterizing graphite stress responses. The classical elasticity has not been able to correlate the various experiments of graphite, but information that can lead to the quantitative verification of the couple-stress theory for graphite is normally missing in the reported data.

In what follows, some representative evidences of nuclear grade graphite beams under pure-bending reported in Refs. 3, 4, and 7 are qualitatively compared with the results of the couple-stress theory. Since some available experimental data are measured for noncircular cylinders, it is assumed that the implications of the circular cylinder obtained in this article is applicable qualitatively, or by an analogy, to the noncircular cylinders with the similar C_t and C_m.

To utilize the results of the previous sections, the apparent flexural stress $\tau_{zz}^{(a)}$ in a beam under pure-bending is defined by

$$\tau_{zz}^{(a)} = - \frac{M_y x}{I_y} \quad , \tag{7-1}$$

where $x = r \cos \theta$ is the distance of the material point from the neutral axis, and M_y is the total moment about the y-axis. With this definition, the bending moment M_y given by Eq. 5-6 yields

$$\tau_{zz}^{(a)} = C_m \frac{Ex}{\rho} \quad . \tag{7-2}$$

This relation makes clear that C_m is equivalent to the quotient

$$\frac{\tau_{zz}^{(a)}}{Ex/\rho}$$

for the couple-stress materials. In the following discussion, these two quantities will not be distinguished, with the understanding that the latter is the parameter implicitly used in most experimental reports (e.g., Ref. 3). Also, $\tau_{zz}^{(a)}$, defined by Eq. 7-1, is not the actual axial stress τ_{zz} which is given by Eq. 5-7.

Based on the loading and the strain measurements (Ref. 3), C_m is independent of the bending curvature for a given graphite beam with unspecified cross section. Quantitatively, C_m is approximately 1.35, which is greater than 1 as required by Eq. 6-4.

No explicit data are available to establish a functional relation between C_m and the beam cross section of nuclear graphite, but it is reported that $\tau_{zz}^{(a)}$ for the graphite beam at failure state decreases with the increase of the beam volume (Ref. 4). This observation suggests that

the measured values of C_m decrease with the increase of the beam cross section and agrees with the characteristics of C_m described in conclusion 4 of Section 6.

A useful relation can be derived from Eqs. 5-7 and 7-2 and conclusion 5 of Section 6:

$$\tau_{zz}^{(a)} > \tau_{zz} \quad . \tag{7-3}$$

This relation shows that the apparent flexural stress is always greater than the actual axial stress for a material with couple-stresses. If the failure of the graphite beam is determined by the maximum tensile stress, then τ_{zz} at failure state equals the uniaxial tensile strength, and Eq. 7-3 yields that the apparent flexural stress of a graphite beam at failure state is higher than its uniaxial tensile strength. This is clearly measured experimentally and stated in Refs. 3, 4, and 7.

Next, use is made of the observation that the maximum failure strain of the pure-bending test exceeds the uniaxial tensile failure strain (Ref. 3) with the presumption that the elastic response of the nuclear grade graphite can be predicted by the couple-stress theory of linear elasticity. Since the measured maximum tensile strain in the pure-bending test is a/ρ, the maximum tensile stress failure criteria and Eq. 5-7 yield that $C_t a/\rho$ at the bending failure equals the uniaxial tensile failure strain, Thus, it is reasonable to extract from the measurements on strains in Ref. 3 that

$$C_t < 1 \quad . \tag{7-4}$$

Employing Eq. 6-1 results in

$$\nu \, (\nu + \bar{d}_2/\bar{d}_1) < 0 \quad . \tag{7-5}$$

for nuclear graphite.

The practical application of the couple-stress theory needs the material constants $\bar{d}_1$ and $\bar{d}_2$ to be determined experimentally. As a result of the solution in this article, it is necessary to measure the cross section, the applied moment, and the bending curvature for a bending test, in addition to the Young's modulus and Poisson's ratio determined by homogeneous deformations. Also, more than one cross section is needed to fully characterize both $\bar{d}_1$ and $\bar{d}_2$. There are no experimental data dictated by the couple-stress theory in current literature. The following estimation of $\bar{d}_1$ and $\bar{d}_2$ serves only as a further evidence that the existing graphite data is compatible with the general aspect of the couple-stress theory.

In analysis of the H-451 graphite data in Ref. 7, the ratio of the uniaxial tensile strength to the apparent flexural stress at the failure state is needed, since these two quantities are measured, and their ratio is used as a parameter in Ref. 7. With the maximum tensile stress failure criteria, this ratio equals C_t/C_m. In the discussion below, this failure criteria is adopted, and the quotient C_t/C_m is used for the ratio of the uniaxial tensile strength to the apparent flexural stress at failure.

For H-451 graphite, it is reported in Ref. 7 that the C_t/C_m ratio ranges from 0.5 to 0.8 for the 6.4-mm-diameter circular cylinder. Theoretical values of C_t/C_m against a/ℓ_2 for $\bar{d}_2/\bar{d}_1 = 0$, as depicted in Fig. 7-1, can be used to calculate ℓ_2, which ranges from 0.53 to 1.12 mm. If $\bar{d}_2/\bar{d}_1 = -0.8$ is chosen so that Eq. 7-5 is satisfied, ℓ_2 falls in the range 0.62 to 1.54 mm from Fig. 7-1. It is obvious that these values of ℓ_2 are at the same order of the grain size of the H-451 graphite (maximum at 1.57 mm). This agrees with the general aspect of the couple-stress theory that Mindlin has described (Ref. 2).

The discussions in this section have shown that the graphite uniaxial and pure-bending test results which are incompatible in the classical beam theory can be accommodated in the couple-stress theory. The conclusion is therefore that the nuclear grade graphite is influenced by couple-stress and that the couple-stress theory may answer why many graphite phenomena are noticed as being discordant with classical elasticity.

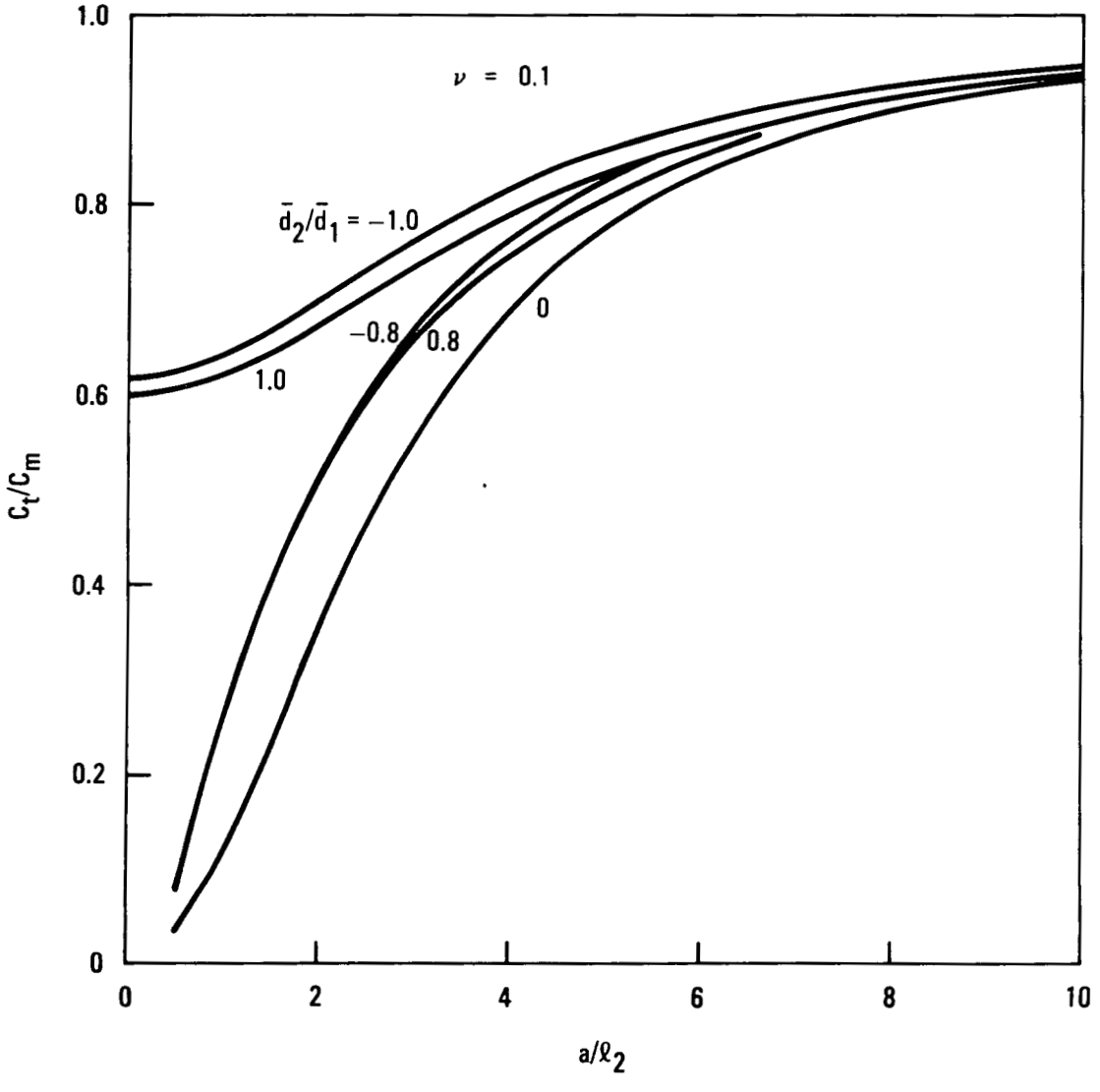

Fig. 7-1. Theoretical ratio of the uniaxial tensile strength to the apparent flexural stress at failure, C_t/C_m, for a circular cylinder subjected to pure bending in the couple-stress theory for Poisson's ratio $\nu = 1$

ACKNOWLEDGEMENT

The authors are indebted to Dr. P. Y. Tang for the valuable discussions and encouragement during the course of this research.

REFERENCES

1. Mindlin, R. D., and H. F. Tiersten, "Effects of Couple-Stress in Linear Elasticity," Arch. Rat. Mech. Anal. 11, 415 (1962).
2. Mindlin, R. D., "Influence of Couple-Stresses on Stress Concentrations," Exp. Mech. 3, 1 (1963).
3. Brocklehurst, J. E., and M. I. Darby, "Concerning the Fracture of Graphite under Different Test Conditions," Mat. Sci. Eng. 16, 91 (1974).
4. Brocklehurst, J. E., "Fracture in Polycrystalline Graphite," Chem. Phy. Carbon 13, 145 (1977).
5. Timoshenko, S. P., and J. N. Goodier, Theory of Elasticity, 3rd ed., McGraw-Hill, New York, 1970.
6. Olver, F. W. J., "Bessel Functions of Integer Order" in Handbook of Mathematic Functions, M. Abramowitz and I. A. Stegun (eds.), Superintendent of Documents, U. S. Government Printing Office, Washington, D. C., 1964, p. 355.
7. Price, R. J., "Statistical Study of the Strength of Near-Isotropic Graphite," ERDA Report GA-A13955, General Atomic Company, May 24, 1976.